



Investigating the effects of electrochemical discharge machining (ECDM) on the dimensional accuracy and surface integrity of the PDMS microchannel

Arsalan Torabi¹ · Mohammad Reza Razfar¹

Received: 10 March 2022 / Accepted: 24 August 2022

Published online: 24 September 2022

© The Author(s) 2022 [OPEN](#)

Abstract

In this study, the electrochemical discharge machining (ECDM) process was used to fabricate a microchannel on polydimethylsiloxane (PDMS), which is able to fabricate channels on the non-conductive materials at low cost and acceptable material removal rate (MRR). One of the main advantages of this method, in addition to much less time and cost, is the possibility of achieving high depths (up to 1000 μm). For this purpose, the effect of electrolyte concentration, rotational speed, feed rate, and machining voltage on the surface quality and surface roughness was investigated in the PDMS micromachining. It was found that the ECDM is capable of fabricating the channels with the surface quality similar to lithography. Also, with increasing the machining voltage and electrolyte concentration, the MRR increases and the possibility of mechanical contact between tool and workpiece decreases. Increasing the machining voltage and also the electrolyte concentration changes the machining regime from contact machining to electrochemical machining. Increasing the machining voltage from 38 to 42 V increases the channel cross-section by nearly 40%. Also, the surface roughness increases by 36% with increasing the voltage from 38 to 42 V. Changing the rotational speed from 0 to 10,000 rpm, due to the reduction in the thickness of gas film, reduces the side sparks and concentration of the sparks on the bottom of the tool, which reduces the surface roughness. The Response Surface Method was used to achieve a mathematical model between inputs and outputs. The model represented a Quadratic Equation to predict the outputs.

Article highlights

- The electrochemical discharge machining (ECDM) process was used to fabricate a microchannel on polydimethylsiloxane (PDMS) with the surface quality similar to lithography.
- Process is able to create the feature in much less time and cost, also achieving high depths (up to 1000 μm) is possible.
- The effect of electrolyte concentration, rotational speed, feed rate, and machining voltage on the surface quality, surface roughness and dimensional accuracy was investigated in the PDMS micromachining.

Keywords Polydimethylsiloxane · Electrochemical discharge machining · Microchannel

✉ Arsalan Torabi, at.arsalantorabi@aut.ac.ir | ¹Department of Mechanical Engineering, Amirkabir University of Technology, Tehran, Iran.



1 Introduction

Glass, ceramics and polymers are among the materials that have been widely used in recent decade in the microfluidics industry. In this industry, there is an increasing need to create complex geometries with small dimensions and high quality [1–3]. The patterns created in glass and ceramics are faced with the problems due to the brittleness [4–6]. This caused that glass and ceramics soon gave way to polydimethylsiloxane (PDMS) in many applications. When PDMS is cured, it behaves like an elastic solid and maintains its molded structure. The use of PDMS in the microfluidic applications was first proposed by Whitesides in the mid-1990s [7, 8]. To date, several other polymer materials such as polyurethane methacrylate (PUMA) and polymethyl methacrylate (PMMA) have been used for the fabrication of microchannels, but PDMS remains the predominant polymer used in the microfabrication of microfluidics. The PDMS microchannels fabricated by the micromolding using the remolding technique have a widespread use.

PDMS is able to limit the detection of short-wavelength fluorescence (about 400 nm). Therefore, for the laser-induced fluorescence (LIF), the PDMS sensitivity is less than glass devices. The selection of PDMS as a short channel material is due to its biocompatibility and simple fabrication using the remolding method [7]. Gelszinnis et al. reported the use of magnetophoresis in the micro-systems using the PDMS-I structures, which are made up of carbonyl iron micro-particles mixed in the PDMS matrix. Zainal Abidin et al. proposed the fabrication and test of PDMS microfluidic channels to separate magnetically-labelled biological cells [9].

Lithography is one of the most common techniques to create a channel in the PDMS [10, 11]. However, this process has some disadvantages, such as the high time and cost of the process, sloped walls, or failure to access the vertical wall. Also, the maximum depth of the channel created by this method is generally less than 200 μm [12, 13]. Microchannels refer to the channels with the cross-section smaller than 1 mm and larger than 1 μm . At the cross-sectional dimensions greater than 1 mm, the fluid flow in the channel will behave similar to the fluid motion on the microscopic scale [14]. Microchannels have many applications and advantages due to the high surface-to-volume ratio and the small volume, some of which were mentioned [15, 16].

The electrochemical discharge machining (ECDM) process, whose schematic is shown in Fig. 1, is able of machining non-conductive materials and first was first used for drilling the them [17–19]. The diameter of the created holes ranges from a few micrometers up to a

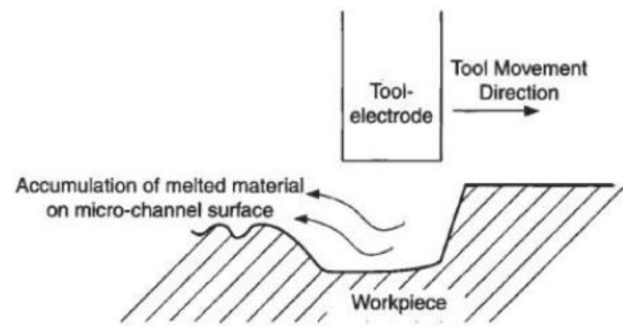


Fig. 1 Schematic of machining operations with electrochemical discharge process

few millimetres [20]. By moving the tool against the workpiece surface, the two-dimensional (2D) and three-dimensional (3D) structures can be created [21, 22]. The first 3D geometries were created by Wüthrich et al. [23]. Furutani et al. then developed the 2D and 3D structures [24]. Most research works in this area have been done by Wüthrich et al. [23, 25].

In a group work, Wüthrich and Fascio created the first 3D structures with an electrochemical discharge process. They used three types of glass with different compositions as workpieces and examined the effect of parameters such as tool distance to workpiece, applied voltage and material of workpiece on the machining depth and channel surface quality. The number of tests performed by the authors were limited and more focused on the feasibility of the machining process [23, 25].

If the tool is considered a source of thermal energy, its movement against the workpiece determines the time the workpiece is subjected to the thermal energy. Therefore, the correct choice of the tool feeding parameter in combination with the voltage level and form (as a representative of the heat source), plays an important role in the quality of the machined surface, dimensional accuracy and heat-affected area [26]. Mehrabi et al. and Sabahi et al. performed experimental and numerical studies on the channel depth in the ECDM process. Accordingly, the best temperature as the material removal temperature was obtained 700 $^{\circ}\text{C}$ [27, 28].

It is observed that it is necessary to achieve surface quality and dimensional accuracy in the microchannels created in the PDMS. Also, the ECDM is able to create the desired geometries in microfluids in the PDMS components. On the other hand, the surface integrity and dimensional accuracy have not been investigated in the ECDM of PDMS. Therefore, the aim of this study was to investigate the ECDM of PDMS to achieve the required surface integrity to be used in the manufacture of biological laboratory equipment. In this study, the microchannels

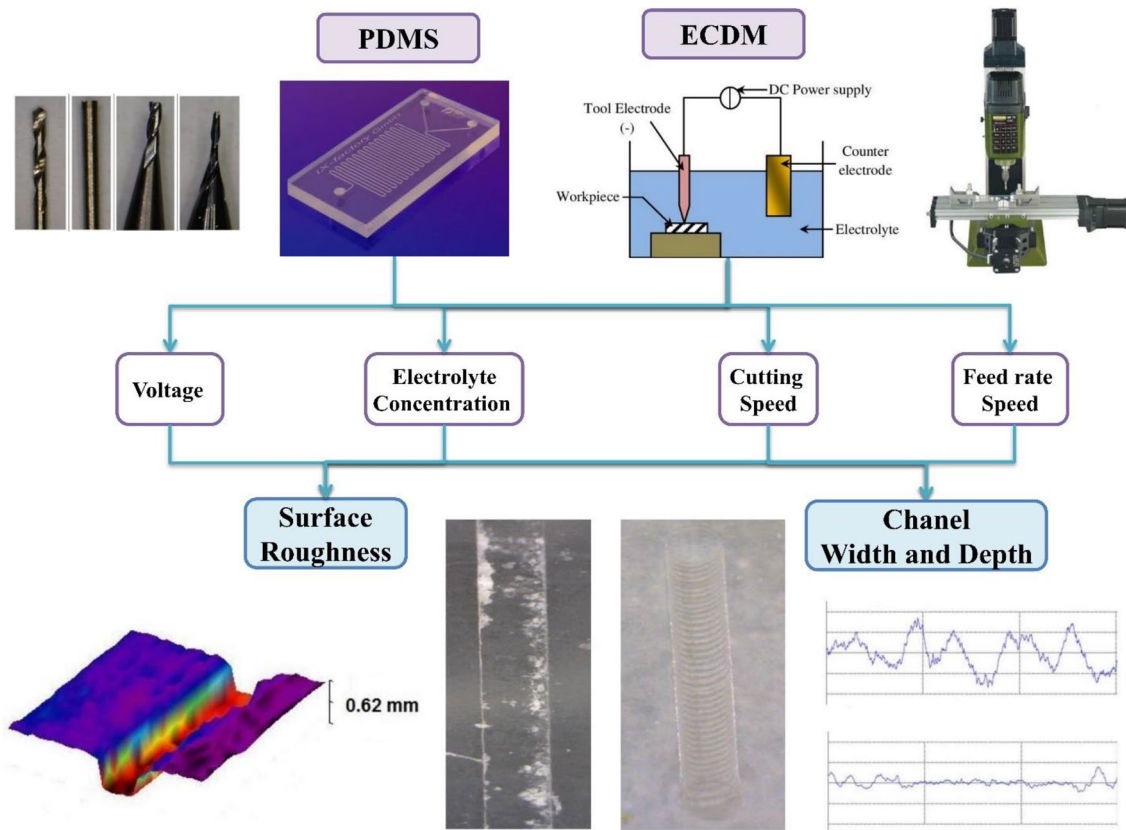


Fig. 2 Research block diagram

were fabricated by the ECDM process on PDMS and the effect of various parameters such as voltage between the two ends of electrodes, electrolyte concentration, and tool feed rate on the channel surface roughness was investigated. The research block diagram is shown in Fig. 2, which illustrates that the research tries to find out that on the PDMS machining using ECDM, how we can improve the surface integrity and dimensional accuracy by controlling the electrolyte concentration, rotational speed, feed rate, and machining voltage.

In the next section, the research method and material specifications is presented. Next, the results are shown and discussed. Finally the main achievements of this research are presented in the conclusion section.

2 Materials and methods

The electrochemical discharge creates the necessary conditions for machining the non-conductive materials by the chemical and electrochemical corrosion principles. Depending on the process, a device should be used to perform the experiments that can provide small-scale precise linear movements in different motion courses.

To perform the experimental tests, the MF70 micromachining device equipped with a KT70 table is used. The motion mechanism of the table operates in the two X and Y directions by the linear movement of the ball screw and stepper motor. The vertical Z axis is used to provide the mechanism for the gravity feeding and to adjust the distance between tool and workpiece.

The manufacturer recommends that the prepolymer and cross-linker be mixed at a 10:1 weight ratio, respectively. In this study, PDMS (Sylgard 184) prepolymer and cross-linker were combined. The tool used in this process is a simple cylindrical tool with a diameter of 0.5 mm. The workpiece used for the ECDM process in this study is a rectangular cube piece made of PDMS with the dimensions of 75×75 mm. The aqueous solution of sodium hydroxide with the weight concentrations of 20, 25 and 30% was used as the electrolyte. After fabricating the channel, the whole piece is cleaned for 15 min in an ultrasonic bath using the distilled water solution, the section is cut with a surgical knife and then examined by an optical microscope. Care should be taken to cut the cross-section so that there is no crushing or deformation at the channel site to avoid the error in the test

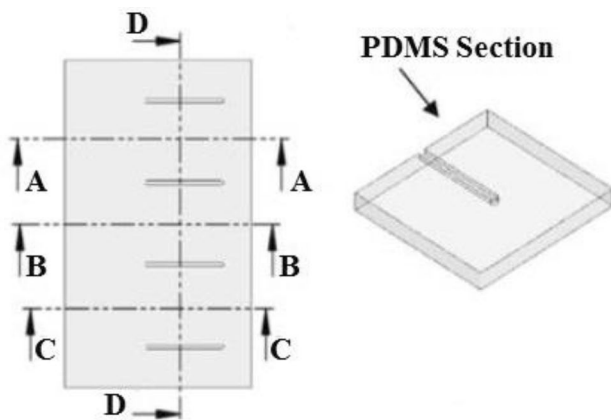


Fig. 3 Cutting cross-section of PDMS piece

results. The methods of cutting the parts and inspecting the cross-section can be seen in Fig. 3.

According to Fig. 3, the piece is first cut with a surgical knife on line D, and after creating section D, the piece is cut in the A, B and C directions. The cross-section of the cut pieces is observed by the Dino-lite digital camera model ZT4113AM and the section dimensions are measured after the camera calibration by the calibration ruler. Also, to measure the roughness of the surface of the channels created by the process on the samples, the digital roughness measuring device (MarSurf PS10-Elcometer7062, Germany) was used. The course length of the probe movement is selected according to the standard based on the roughness range expected from this process [29, 30]. According to the standard for measuring the roughness, the roughness tests are repeated five times and the reported values are the average of the measured values. To avoid the test error and ensure the process repeatability, the tests are repeated two to three times. Finally, the surface of the created channels is examined by the laser profilometer.

As is discussed in the literatures, electrolyte concentration, rotational speed and feed rate, and applied machining voltage are of the most effective ECDM process parameters. The range of input parameters are selected using the literature suggested values or achievable values using devices. In this study, the effect of the main input parameters (electrolyte concentration, rotational speed and feed rate, and applied machining voltage) on the surface roughness, surface quality and dimensional accuracy was investigated. By reviewing the literatures and some initial test, the condition which results in no material removal or unstable material removal was determined as higher and lower values of parameters along with an average value. The tests were performed as the complete factorial (a total of 54 experiments) and the levels of constant and variable parameters are presented in Table 1.

Table 1 Levels of input parameters of experimental tests

Parameter	Value		
	Level 1	Level 2	Level 3
Voltage (V)	38	40	42
Electrolyte concentration	20%	25%	30%
Spindle speed (rpm)	0	5000	10,000
Feed rate speed (mm/min)	0.6	1.2	–
Electrolyte	NaOH		
Tool material and diameter	Flat head HSS, 0.5 mm		
Electrolyte volume	800 cc		
Tool submerged depth	1.5–2 mm		
Electrolyte temperature	25 C		

3 Results and discussion

3.1 Surface roughness

After the initial tests, the first voltage leading to the complete channel on the sample was 38 V. The effect of machining voltage on surface roughness (R_a) is shown in Fig. 4 and Appendix Fig. 18. It was observed that using the voltage of 38 V, assuming that the other parameters are kept constant, the surface roughness is obtained greater than the two voltages of 40 and 42 V. The reason for this increase in roughness is the predominance of the material removal mechanism over the loading mechanism by the electrochemical discharge.

In the study of Abou Ziki et al. [31], it was suggested that machining in this area causes the effect of tool contact on the bottom of machined channels. This effect, known as the stick-jump effect, indicates that the tool length increases due to the process nature and increase in tool temperature, and proportional to the distance between the tool and the workpiece and the horizontal speed of the tool, the stick-jump effect on the channel surface is shown in Fig. 5.

As shown in Fig. 5, the tool penetrates into the workpiece due to the expansion. After the horizontal movement of the tool, as the tool sticks to the soft polymer, the tool makes an angle (α) and by continuing the horizontal movement of the tool, it is separated from the workpiece (c). After the angle of the tool reaches a certain value, due to the softness of the polymer, the tool jumps and moves to another place and becomes horizontal and a new hole is created (d and e) [31].

The mechanism of sticking and jumping the tool out of the workpiece in this study is similar to the observations of Abou Ziki et al., except that in the case where the tool rotates, a specific motion can be observed in the tool. The low operating voltage and also the diluted electrolyte solution can lead to such effects. In other words, the

Fig. 4 Effect of machining voltage and rotational speed on surface roughness in different conditions; **a** $V_f = 1.2$ mm/min - NaOH-30%. **b** $V_f = 0.6$ mm/min - NaOH-30%. **c** $V_f = 1.2$ mm/min - NaOH-25%. **d** $V_f = 0.6$ mm/min - NaOH-25%

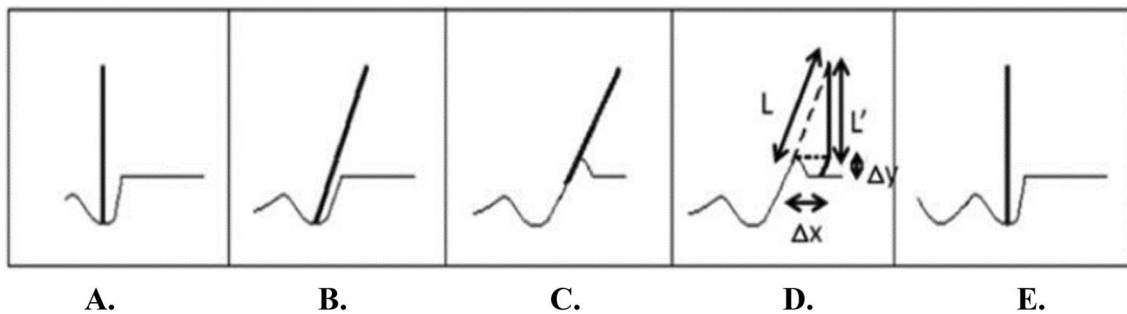
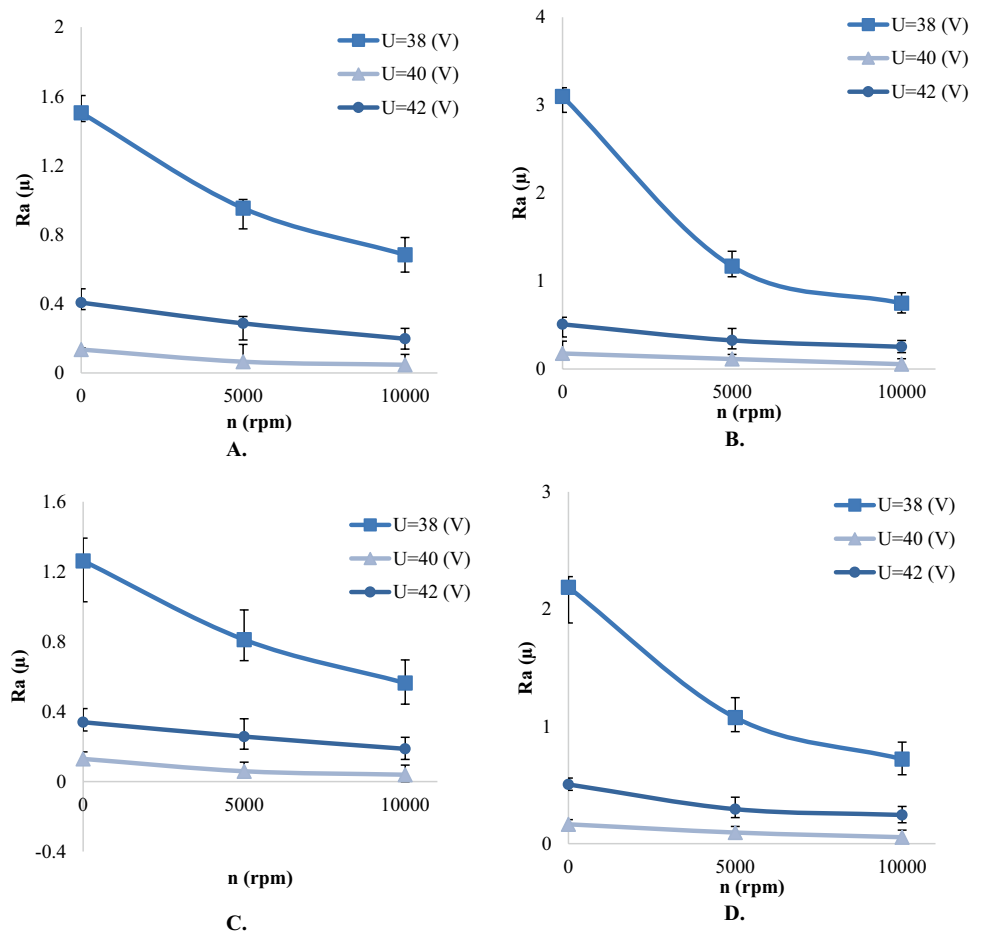


Fig. 5 Mechanism of tool sticking and jumping out of workpiece for creating channel with electrochemical discharge process: **a** Expansion and penetration of tool into workpiece, **b** Sticking of

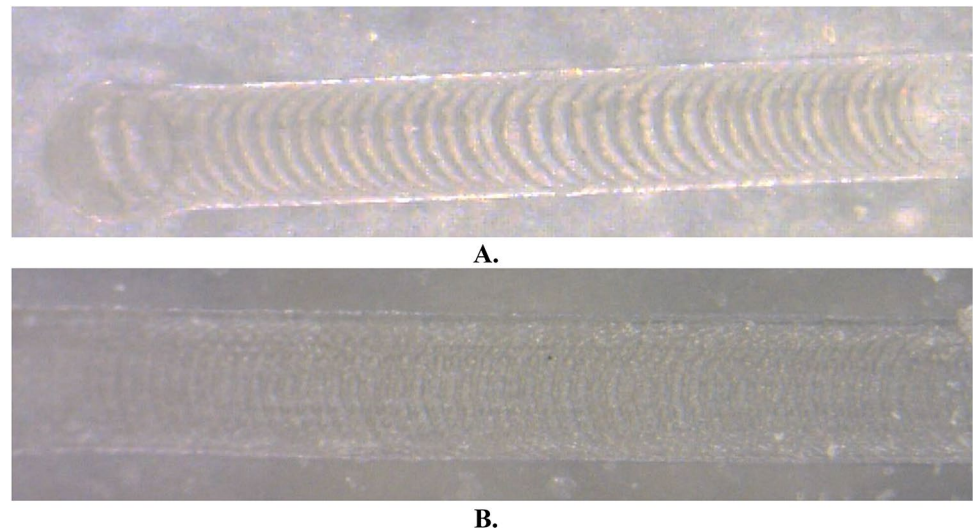
tool to piece, **c** Sticking and separation of tool from workpiece surface, **d** Bending and jumping of piece to another place, **e** Formation of another hole

predominance of material removal over electrochemical discharge leads to these effects, reducing the surface quality and increasing the roughness. 0 shows the effect of voltage on the form and roughness of the surface. As can be seen in 0, at 38 V, the predominant unloading mechanism is the mechanical contact of tool and workpiece. However, at 40 V, the two mechanisms of material removal and electrochemical discharge are balanced. Given that

the channel dimensions are larger than the tool dimensions at 42 V, it can be concluded that the predominant unloading mechanism at 42 V is the electrochemical discharge mechanism.

Due to the higher spark energy at 42 V than that at 40 V and 38 V for each spark, the location of the spark effect and the volume of the loaded material increase. For this reason, the surface roughness in 42 V is higher than that

Fig. 6 Effect of rotational speed on tool movement at 38 V, feed rate of 0.6 mm/min, 25% concentration and rotational speeds of **a** zero and **b** 5000 rpm



in 40 V, and its use is not recommended due to the higher surface roughness and the larger channel dimensions, as described below.

0 shows the surface roughness profile at 38, 40 and 42 V for the zero rotational speed, 25% concentration and 0.6 mm/min feed rate. The surface roughness at 38, 42 and 40 V is in the ranges of 0.32–0.55, 0.18–0.54 and 0.03–0.18 μm , respectively.

Figures 4 and 6 and Appendix Fig. 19 shows the effect of rotational speed on tool movement at 38 V, 0.6 mm/min feed rate, without spindle rotational speed, and 25% concentration of electrolyte solution. Rotating the tool at speeds above 25 rpm leads to the turbulence in the gas film around the tool [31, 32]. Rotating faster than this speed will reduce the thickness of the gas film around the tool. By reducing the thickness of the gas film around the tool, the flying sparks emitted from the tool wall and the workpiece surface are reduced. Reducing the sparks along with creating a more regular spark column than the case without rotation leads to a channel with a lower surface roughness. 0 shows the effect of rotational speed changes on the surface roughness of the channels created in the conditions of 38 V voltage, 25% solution of NaOH electrolyte and feed rate of 0.6 mm/min.

In this study, three electrolyte solutions with concentrations of 20, 25 and 30% were used, and their effect on the surface roughness is shown in Fig. 7 and Appendix Fig. 20. In the electrolyte with lower concentration (20%), due to the low power of this solution in chemical etching, the surface texture is not well corroded, which leads to the effect of tool movement on the surface of the channels. In the electrolyte with higher concentration (30%), the high energy of the sparks along with the high corrosive power

of the electrolyte causes the damage to the channel surface and increases the surface roughness.

The reason for the increase in the spark energy can be attributed to the stability of the gas film. The stability of the gas film in electrolyte also depends on the speed at which the bubbles move in the solution, as the faster the upward movement of bubbles, the more unstable the gas film. According to Fig. 8, the forces applied to the bubble are the two gravitational (capillary) and buoyancy forces. The amount of gravitational force applied to this bubble is a constant value, but the amount of buoyancy force (F_B) can be calculated according to Eq. (1) [32]:

$$\frac{4}{3}\pi R_b^3 \rho = F_B, \quad (1)$$

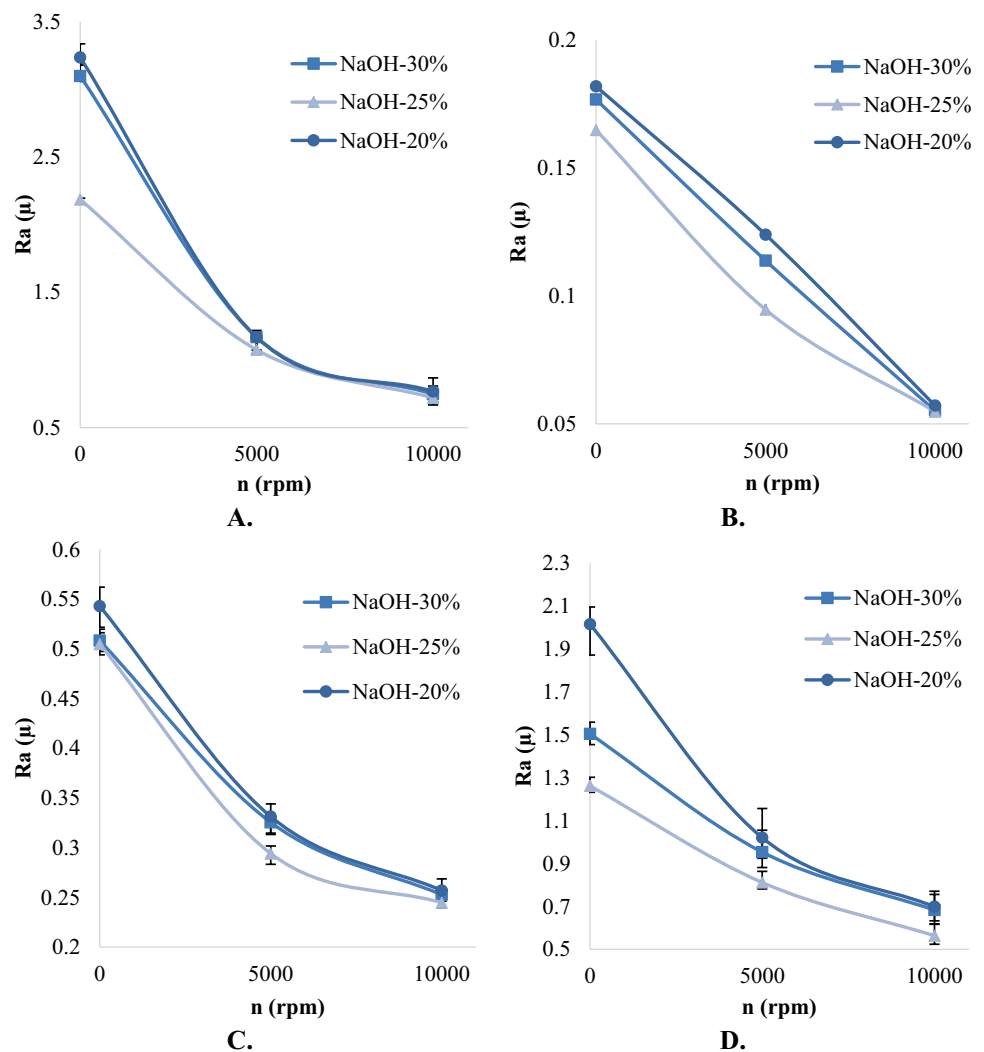
where ρ is the electrolyte density and R_b is the bubble radius and F_B is buoyancy force. On the other hand, when a bubble with the radius of R_b moves inside a viscous fluid with speed v and dynamic viscosity μ , according to the Stokes' law, the frictional force (F_d) is applied to the bubble according to Eq. (2). If dynamic viscosity is replaced by kinematic viscosity, Eq. (2) is obtained:

$$F_b = 6\pi R_b \mu = 6\pi R_b \gamma, \quad (2)$$

where γ is the kinematic viscosity and μ is the dynamic viscosity. As the electrolyte concentration increases, the electrolyte density and viscosity increase. According to Eq. (2), the amount of F_b increases, and it becomes more difficult for the bubble to move within the electrolyte solution [32].

The more stable the gas film, the less time is devoted to the formation of the gas film out of the entire machining process, and the longer time is provided for the discharge electricity, and consequently, the higher the spark energy

Fig. 7 Effect of electrolyte concentration on surface roughness in different conditions. **a** $V=1.2$ mm/min - $U=38$ V. **b** $V=1.2$ mm/min - $U=40$ V. **c** $V=1.2$ mm/min - $U=42$ V. **d** $V=0.6$ mm/min - $U=38$ V



[33]. As mentioned earlier, an increase in spark energy leads to more unloading per spark, resulting in lower surface quality. 0 shows the effect of changes in concentration on the surface roughness of the channels created in the voltage conditions of 38 V, feed rate of 0.6 mm/s and rotational speed of zero.

In this study, two feed rates are considered for the tool (0.6 and 1.2 mm/min) whose effect on the surface roughness in different conditions is shown in Fig. 9 and Appendix Fig. 21. According to previous research, there are two common methods for creating the channels with ECDCM process on the workpiece [32]. In the first method, the tool is placed at a certain close distance from the workpiece surface, and then, without any contact between the tool and the workpiece, the tool travels horizontally along the workpiece surface and the channels are created due to the electrochemical discharge process. In some of the

research work, Didar et al. considered the initial distance between the tool and the workpiece to be equal or more than 15 μ m and used this method to create a channel [34]. In addition, some authors suggested that the ECDCM machining process is able to create a hole or channel on the workpiece if the distance between the tool and the workpiece is less than 25–20 μ m [32]. In some references, it was argued that with the start of the ECDCM machining process, a hole is first created in the piece and the tool penetrates slightly into the piece (performing a vertical feeding) and then, the horizontal feeding of the tool is performed. In some experiments performed by Fascio et al., it was reported that the tool first penetrates 60 μ m into the piece and then, the horizontal feeding is done to create a channel [25].

In the cases where the initial distance of the tool from the workpiece surface is very small (the tool is set on the

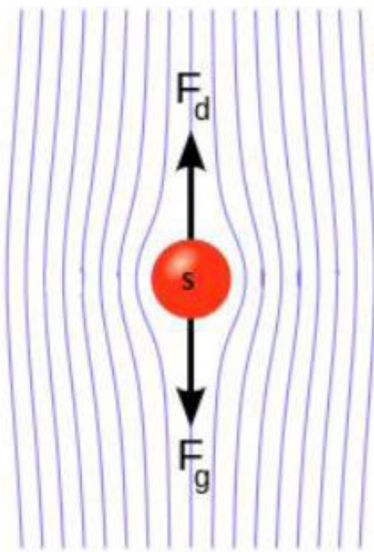


Fig. 8 Schematic of forces exerted on gas bubble immersed in electrolyte solution; F_d frictional force, F_g gravitational force

workpiece surface with a small distance), in the initial ECDM machining process, the tool can penetrate into the workpiece proportional to the process parameters due to the thermal expansion of the tool [25]. Considering the mechanical contact between the tool and the workpiece, it is necessary to adjust the horizontal feed rate of the tool in a suitable way in the machining with ECDM process by selecting other effective parameters in the process. If the tool feed rate is higher than the unloading rate, the tool and the workpiece come into contact with each other, and as a result of this contact, a bending force is applied to the tool which can reduce the surface quality and even lead to the failure of the tool. Figure 10 schematically shows how the tool and the workpiece come into contact during the electrochemical discharge process. On the other hand, if the feed rate of the tool is very low, the machining time increases, which can extend the heat-affected area.

The amount of roughness measured by the roughness measuring device at the feed rate of 10 $\mu\text{m/s}$ is less than the roughness of the measured surface at the feed rate of 20 $\mu\text{m/s}$. The reason for this can be explained by the gas film around the tool. At the slower feed rate, because the tool moves in a halo of gas, the gas film around the tool generates less energy sparks than that at a faster rate, and the sparks with the less energy create a channel with better surface roughness. 0 shows the effect of changes in feed rate on the surface roughness of the channels created

in the conditions of 38 V voltage, 25% solution of NaOH electrolyte and zero rotational speed.

3.2 Channel dimensions

In the electrochemical discharge processes, as the channel depth increases, the conditions become more difficult for reaching the electrolyte to the machining site. When there is fewer electrolytes in the machining area, the unloading rate decreases. For this reason, the machining areas are divided into two areas based on the depth of machining: (1) machining operations at depths less than 250–300 μm : This area is known as the machining area in the electric discharge regime; (2) machining at depths more than 250–300 μm : is known as hydrodynamic machining area. In this area, due to the difficulty of reaching the electrolyte to the tool, the unloading is done slowly, while in the gravity feeding method, a downward force is applied to the tool, which gently moves the tool into the workpiece.

At shallower depths, the electrolyte easily reaches the machining area, and the removal of the corroded materials and continued chemical etching are more easily done. Due to the electric sparks striking the workpiece, which locally increases the temperature and reduces the material viscosity, the chemical corrosion occurs in a more favorable environment.

In this area, the electric sparks are the main determinant of the material removal rate (MRR) and thus, it is stated that machining is underway in the electric discharge regime. In the machining operation as performed in this study, the conduction of electrolyte to the machining area is easily done and, therefore, the machining operation is performed in the electric discharge regime. According to Eq. (3), the average amount of thermal energy of spark (q^*) can be calculated:

$$q^* = UI - RI^*, \quad (3)$$

where U is the applied machining voltage, I is the average current intensity, and R is the inter-electrode resistance. In other words, the energy of each spark is the average energy difference given to the system, part of which is reduced by the inter-electrode resistance from the system. The energy generated by the spark increases the temperature of the tool, workpiece and electrolyte [32]. In this section, the effect of each of the process input parameters on the dimensions of the created channels is examined.

As mentioned earlier, the first voltage that leads to the formation of a complete channel with low or without burr was 38 V. At this voltage, the gas film around the tool grows so that it would produce the sparks at the bottom

Fig. 9 Effect of feed rate on surface roughness in different conditions. **a** NaOH-30% - U=38 V. **b** NaOH-30% - U=40 V. **c** NaOH-30% - U=42 V. **d** NaOH-25% - U=38 V

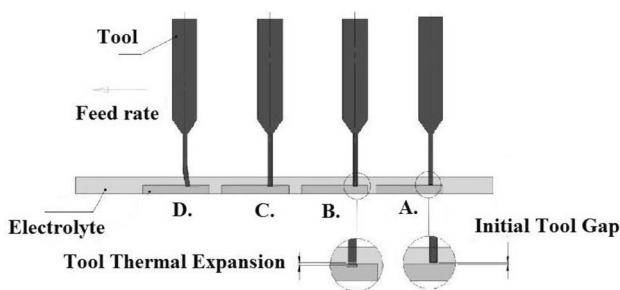
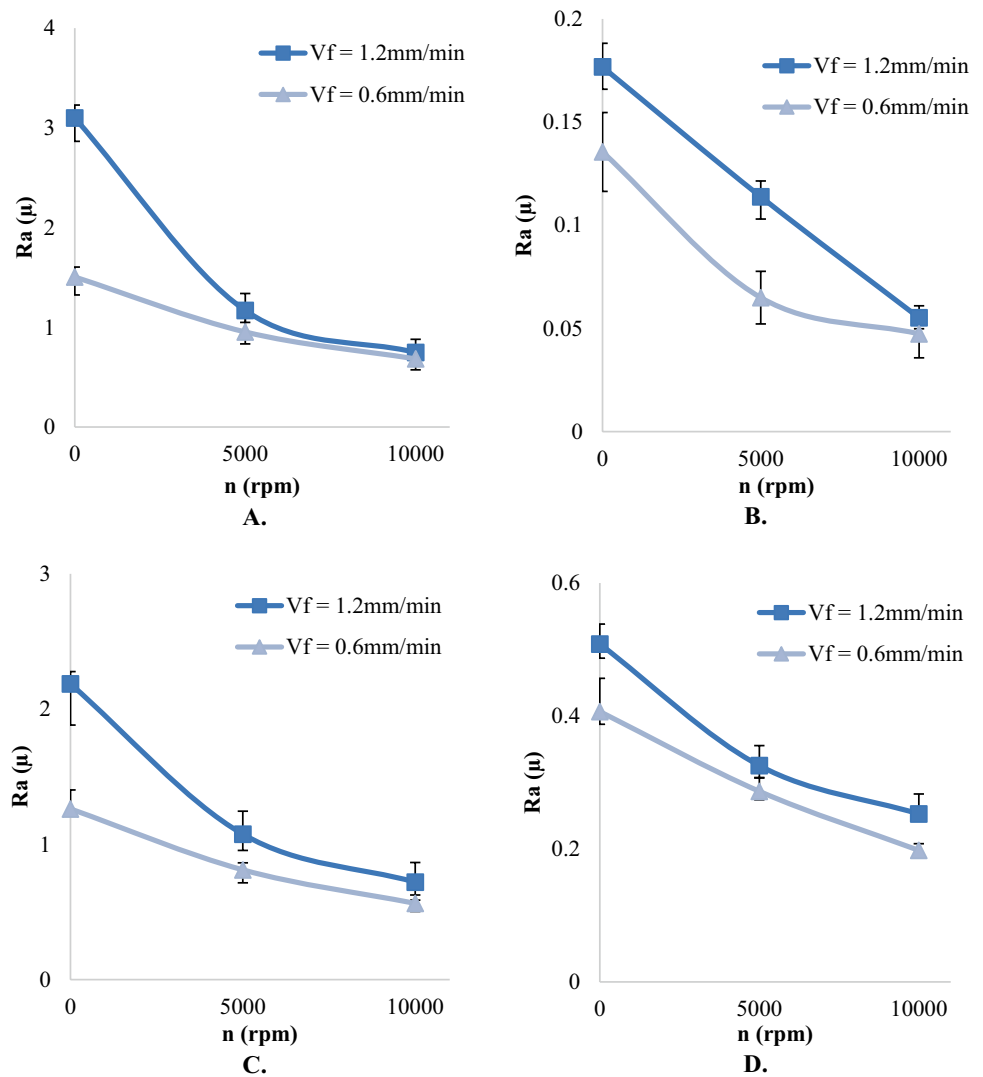
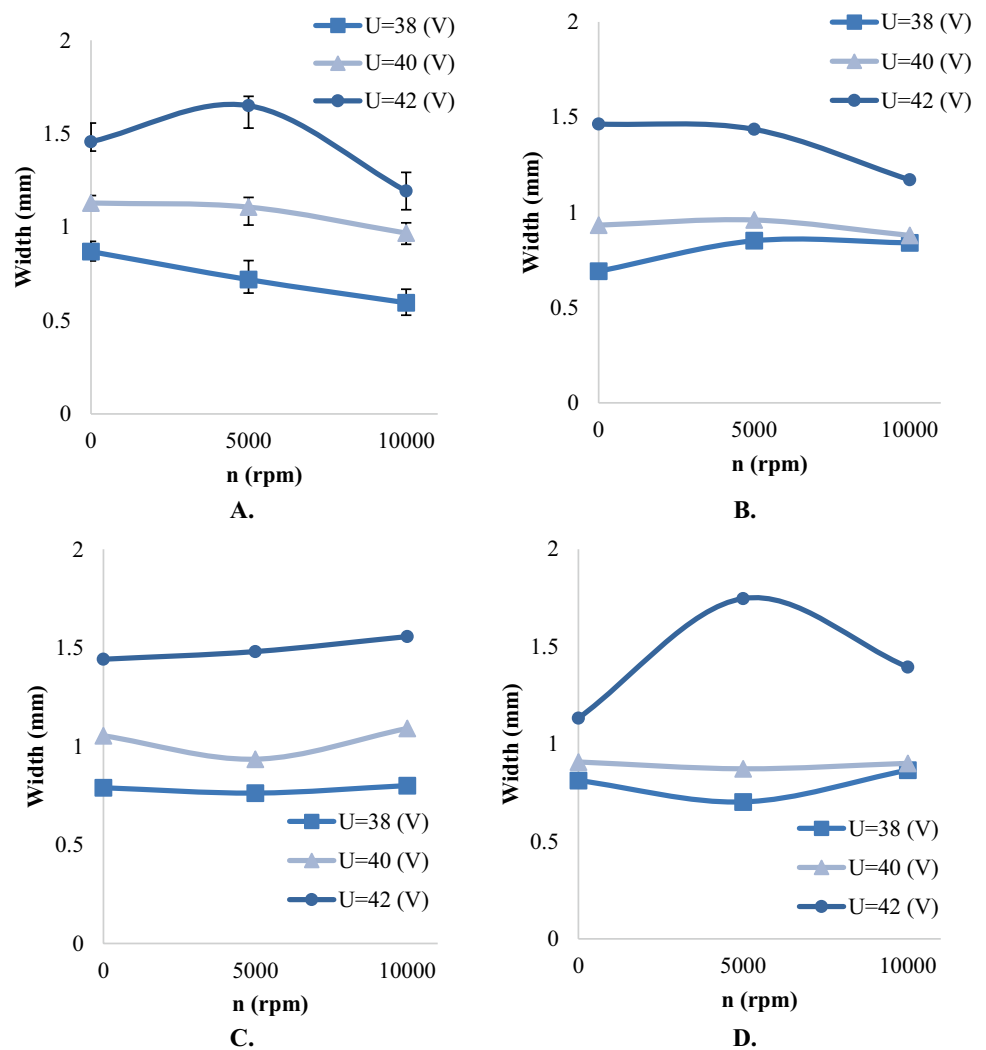


Fig. 10 Schematic view of tool contact with workpiece, **a** before start of machining process, **b** when process starts, **c** performing horizontal feeding, **d** feed rate more than material remove rate

and surrounding the tool. The sparks produced around the tool will cause the flying sparks around the tool, and striking the spark with the workpiece will result in the unloading around the channel and enlarging the channel width.

Due to the fact that the increase in voltage leads to the increase in the flying sparks, the increase in the voltage will also increase the channel width. On the other hand, the presence of the sparks struck from the bottom of the tool to the workpiece plays a major role in the channel unloading and determines the channel depth. Increasing the depth of the channel. The effect of machining voltage on channel dimension is shown in Figs. 11 and 12.

Fig. 11 Effect of machining voltage and rotational speed on microchannel width in different conditions. **a** V=1.2 mm/min - NaOH-30%. **b** V=0.6 mm/min - NaOH-30%. **c** V=1.2 mm/min - NaOH-25%. **d** V=0.6 mm/min - NaOH-25%



In order to facilitate the comparison of the amount of unloading performed in the machining process using the electrochemical discharge, a parameter as the unloaded area is introduced according to Eq. (4). This value is actually the unloaded volume, but due to the fixed length of the channel in all experiments, the unloaded area (s) parameter is introduced by dividing the unloading volume by the channel length. This is the section of channel which can be calculated as:

$$s = w \times h, \tag{4}$$

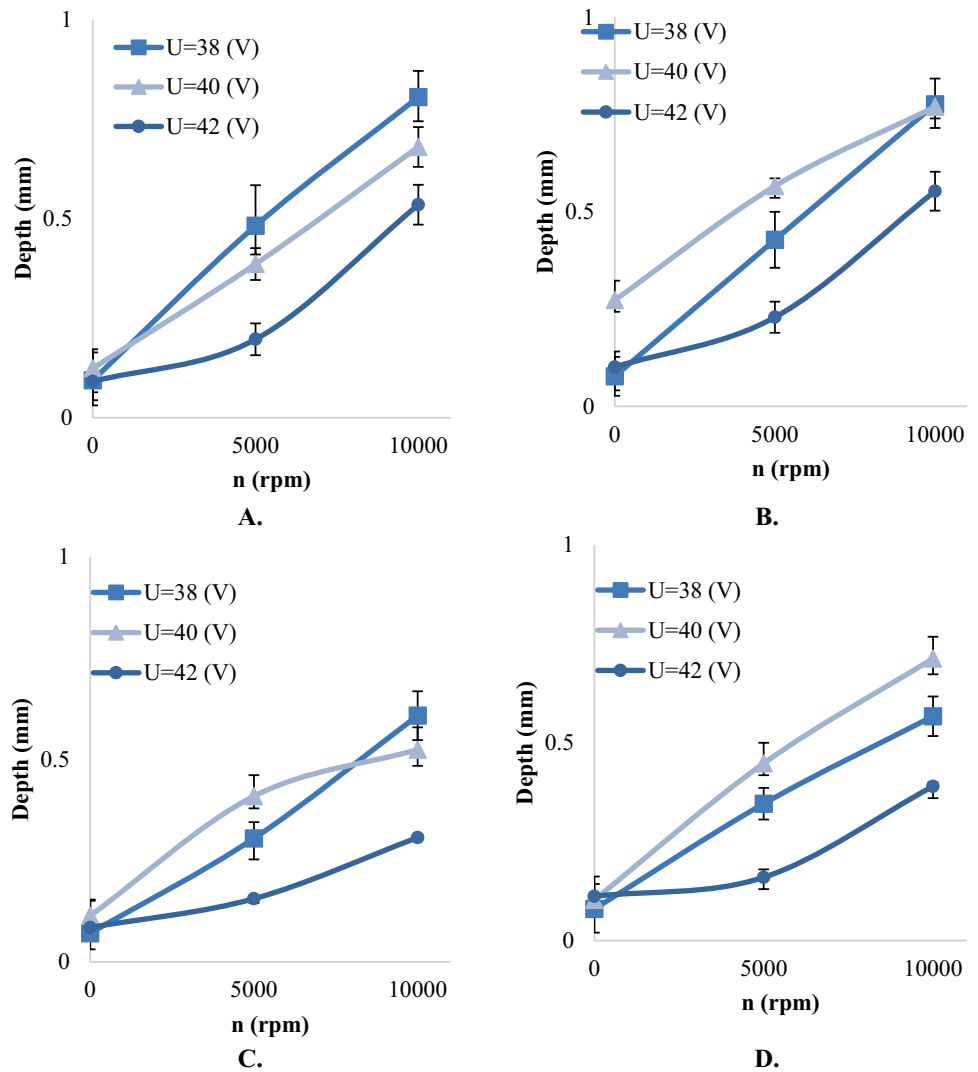
where h is the channel depth and w is the channel width. Figure 13 shows an image taken by an optical microscope from the channels created at zero rotational speed, 0.6 mm/min feed rate, NaOH electrolyte solution with 25% concentration and voltages of 38, 40 and 42 V.

3.3 Comparison between lithography and ECDM methods

As mentioned earlier, lithography is one of the most common ways to fabricate a channel in the PDMS. Therefore, Fig. 14 compares the surface roughness of the channel created by lithography with that of the channel created by ECDM in the best case. It can be seen that the surface roughness of the channel created by ECDM is less than 12% more than that in the lithography method, and due to other advantages of ECDM method such as much less production time and cost, it indicates that the ECDM method can be a very suitable alternative to create the pattern in PDMS. The profiles of the channels created by the two methods are also shown in Fig. 15. The SEM¹ micrograph of fabricated channels using two methods (Lithography and

¹ Scanning Electron Microscope (SEM).

Fig. 12 Effect of machining voltage and rotational speed on microchannel depth in different conditions. **a** V= 1.2 mm/min - NaOH-30%. **b** V= 0.6 mm/min - NaOH-30%. **c** V= 1.2 mm/min - NaOH-25%. **d** V= 0.6 mm/min - NaOH-25%



ECDM) presented in the Fig. 16. It is clearly observed that however the Lithography is able to fabricate more smooth channels, the ECDM is able to create channels with higher depth and higher aspect ratio.

3.4 Statistical analysis

The Response Surface Method (RSM) was used to achieve a mathematical model between four inputs [V_w (Feed rate), n , V , and ρ] and three outputs [surface roughness (R_a), Channel Width, Channel Depth]. The model represented a Quadratic Equation to predict the outputs (Eqs. 5, 6, 7). The minimum value of R^2 (Table 2) was more than 0.81 which confirms the accuracy of model. The diagram of effect of inputs on the surface roughness (R_a) and channel dimension are shown in the Fig. 17.

$$\begin{aligned}
 R_a = & 65.33699 + 11.11295 * V_w - 0.294639 * \rho - 0.001797 * n \\
 & - 2.8339 * V - 0.016912 * V_w * \rho - 0.000116 * V_w * n \\
 & - 0.278353 * V_w * V + 0.00000167342 * \rho * n \\
 & + 0.003565 * \rho * V + 0.000037 * n * V + 0.434101 * V_w^2 \\
 & + 0.002409 * \rho^2 + 0.0000000286433 * n^2 + 0.031719 * V^2
 \end{aligned}
 \tag{5}$$

$$\begin{aligned}
 \text{Channel Width} = & -3.974170.029074 * V_w + 0.001581 \\
 & * \rho - 0.000004125 * n + 0.12421 * V
 \end{aligned}
 \tag{6}$$

$$\begin{aligned}
 \text{Channel Depth} = & 0.552426 - 0.011667V_w + 0.0124 * \rho \\
 & + 0.000043 * n - 0.018683 * V
 \end{aligned}
 \tag{7}$$

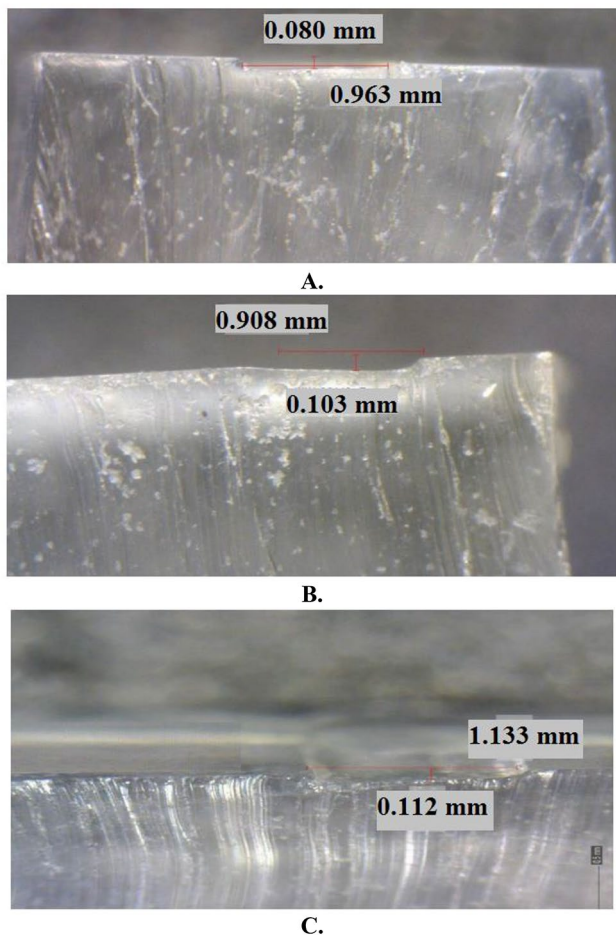


Fig. 13 Effect of voltage changes on dimensions of channels created in process in conditions of zero rotational speed, feed rate of 0.6 mm/min, NaOH electrolyte solution with 25% concentration and voltages of **a** 38 V, **b** 40 V and **c** 42 V

4 Conclusion

In this study, the effect of machining and electrochemical discharge parameters such as the effect of electrolyte concentration, rotational speed and feed rate, and applied machining voltage on the surface quality and surface roughness was investigated. The results of this study can be summarized as follows:

- The ECDM method is capable of creating the channels where the surface roughness of the created channel differs from that of the channel created by lithography by less than 12%. Therefore, considering the other advantages of ECDM method such as much less production time and cost and possibility of achieving high microchannel depth, it can be concluded that the ECDM method can be a very suitable alternative for creating the pattern in PDMS.
- The more stable the gas film, the less the time out of the whole machining process devoted to form the gas film, and the more the time for the electric discharge, resulting in more spark energy. Increasing the spark energy leads to more unloading per spark, resulting in lower surface quality.
- The effect of increasing the machining voltage on the average maximum feed rate is greater than the effect of increasing the electrolyte concentration. At the 38 V voltage, the predominant unloading

Fig. 14 Comparison of surface roughness of channel created by lithography with channel created by ECDM in best case

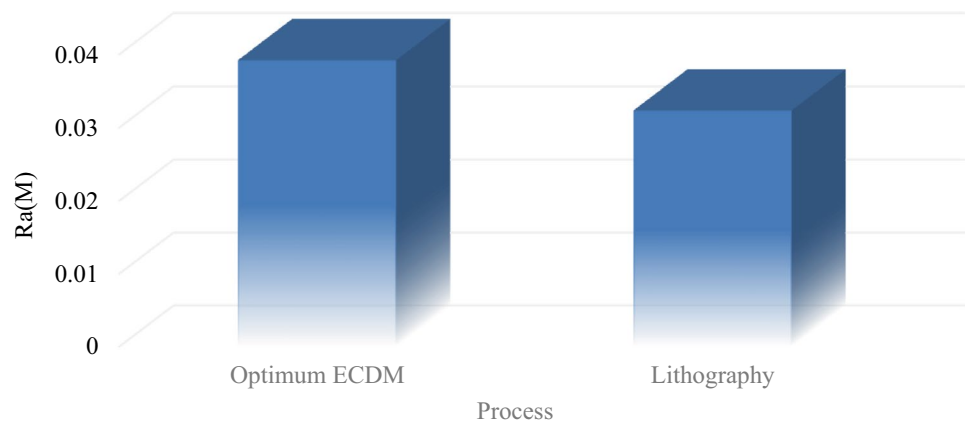


Fig. 15 Comparison of micro-channel profile created by lithography with that created by ECDM in best case; **a** Lithography, **b** ECDM

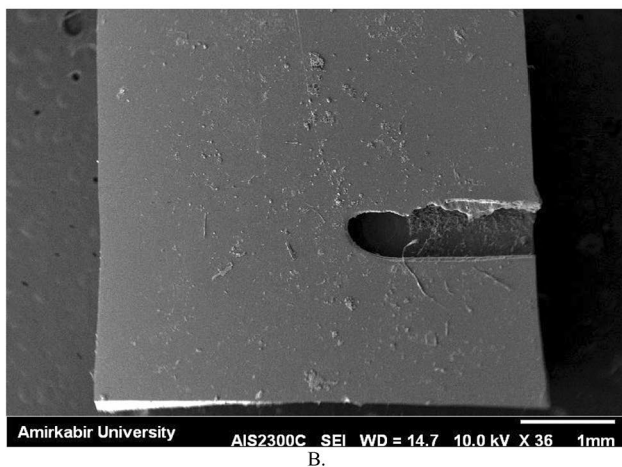
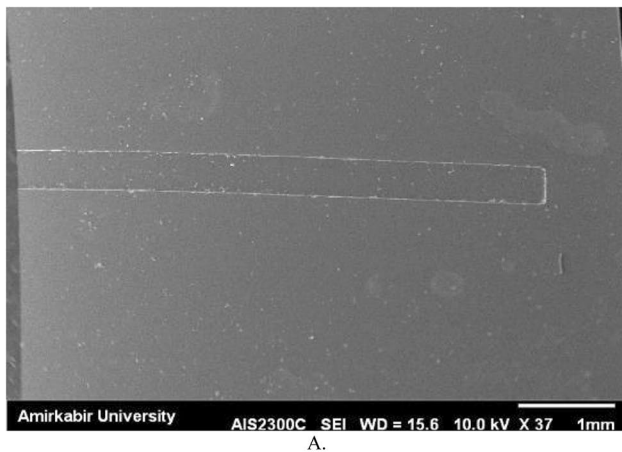
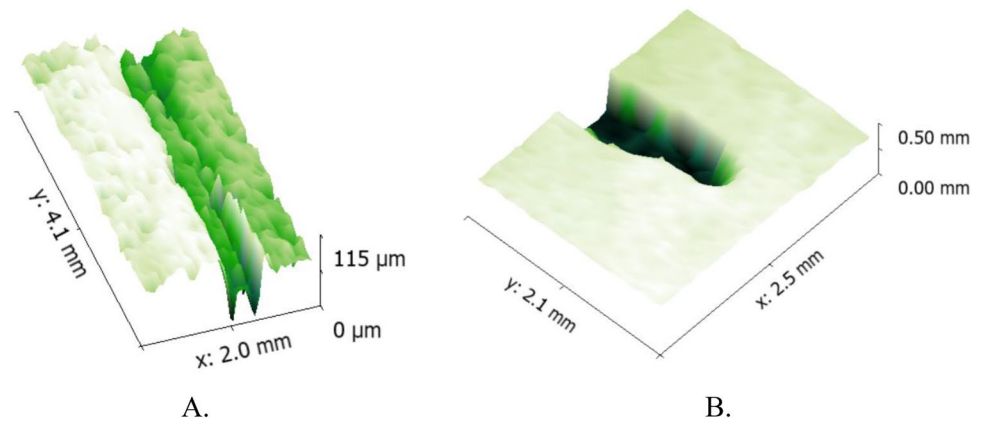


Fig. 16 Comparison of SEM micrograph of microchannel fabricated by lithography and ECDM in best case; **A** Lithography, **B** ECDM

mechanism is the mechanical contact between the tool and the workpiece, but at 40 V, the two material removal and electrochemical discharge mechanisms are balanced. Given that the channel dimensions are larger than the tool dimensions at 42 V, it can be concluded that the predominant unloading mechanism at 42 V is the electrochemical discharge mechanism. By increasing the machining voltage and electrolyte concentration, the MRR increases and the possibility of the mechanical contact between the tool and the workpiece decreases.

- The concentration of the solution generally affects as the both effects of chemical etching on the dimensions of the channels created and concentration on the spark energy, and the spark intensity affects the dimensions of the channels created by the ECDM process.
- The unloading is mainly caused by the sparks created from the bottom of the tool, and the flying sparks essentially increase the channel width.

Table 2 The R² value for outputs

Output	R ²
Ra	0.8716
Width	0.8126
Depth	0.8915

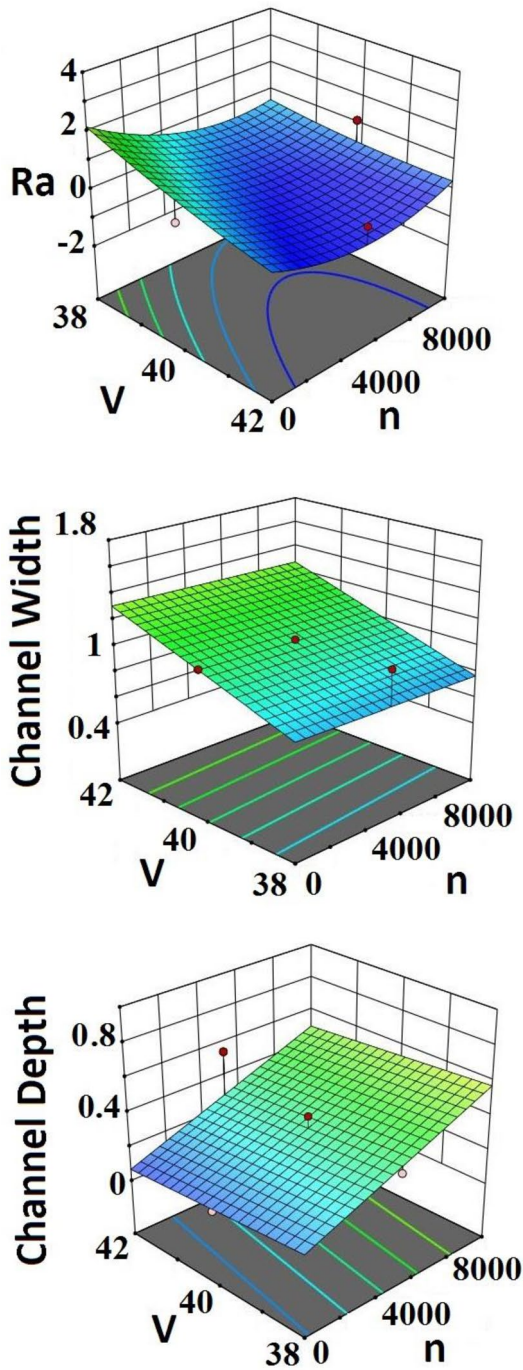


Fig. 17 3D diagram of effect of inputs on Ra and channel dimension

- The effect of ultrasonic vibration on the surface quality of PDMS machined surface using ECDM was not investigated in this research.

- Investigating the effect of using an electromagnetic field in the machining of PDMS using ECDM could extend the application of ECDM in creating PDMS microchanells.

Author contributions Torabi conceived the study, conducts the experiments and prepared the primary manuscript. Razfar supervised the research and critically revised the manuscript.

Funding This research received no specific grant from any funding agency.

Data availability The data sets used and/or analysed during the current study are available from the corresponding authors on reasonable request.

Code availability There is no code or costume made software.

Declarations

Conflict of interest Authors declare no conflict of interest.

Consent to participate The Consent for participate is not applicable for this research.

Consent for publication The Consent for publication is not applicable for this research.

Research involving human and/or animals participants This article does not contain any studies with human participants or animals of which any one of the authors is responsible.

Open Access This article is licensed under a Creative Commons Attribution 4.0 International License, which permits use, sharing, adaptation, distribution and reproduction in any medium or format, as long as you give appropriate credit to the original author(s) and the source, provide a link to the Creative Commons licence, and indicate if changes were made. The images or other third party material in this article are included in the article's Creative Commons licence, unless indicated otherwise in a credit line to the material. If material is not included in the article's Creative Commons licence and your intended use is not permitted by statutory regulation or exceeds the permitted use, you will need to obtain permission directly from the copyright holder. To view a copy of this licence, visit <http://creativecommons.org/licenses/by/4.0/>.

Appendix

See Figs. 18, 19, 20, and 21.

Fig. 18 Effect of voltage changes in channels created under conditions of zero rotational speed, 25% concentration and feed rate of 0.6 mm/min at voltages **a** 38 V, **b** 40 V and **c** 42 V

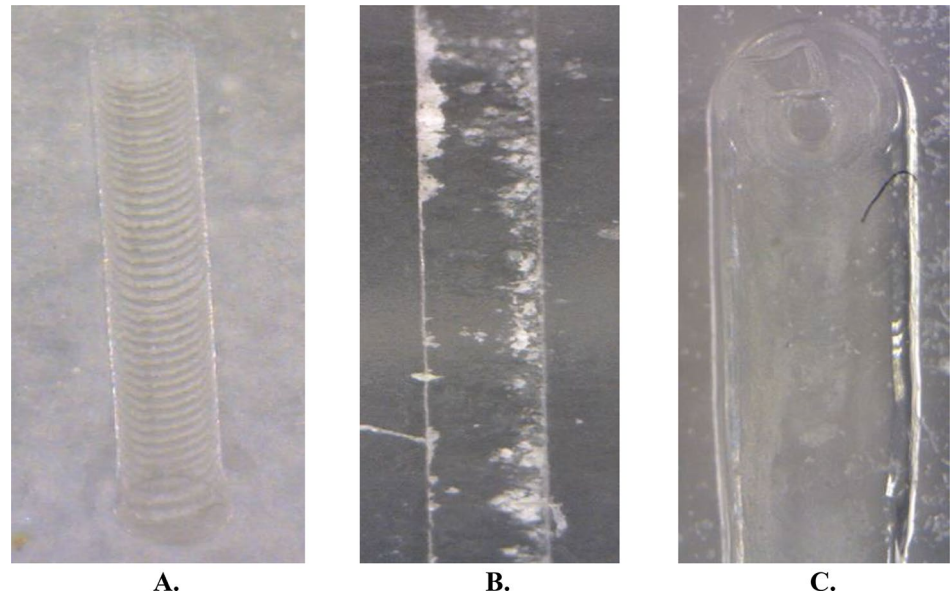


Fig. 19 Surface roughness profile of channels created in voltage conditions of 38 V, NaOH electrolyte solution concentration of 25%, feed rate of 0.6 mm/min and rotational speeds of **a** zero, **b** 5000 rpm and **c** 10,000 rpm

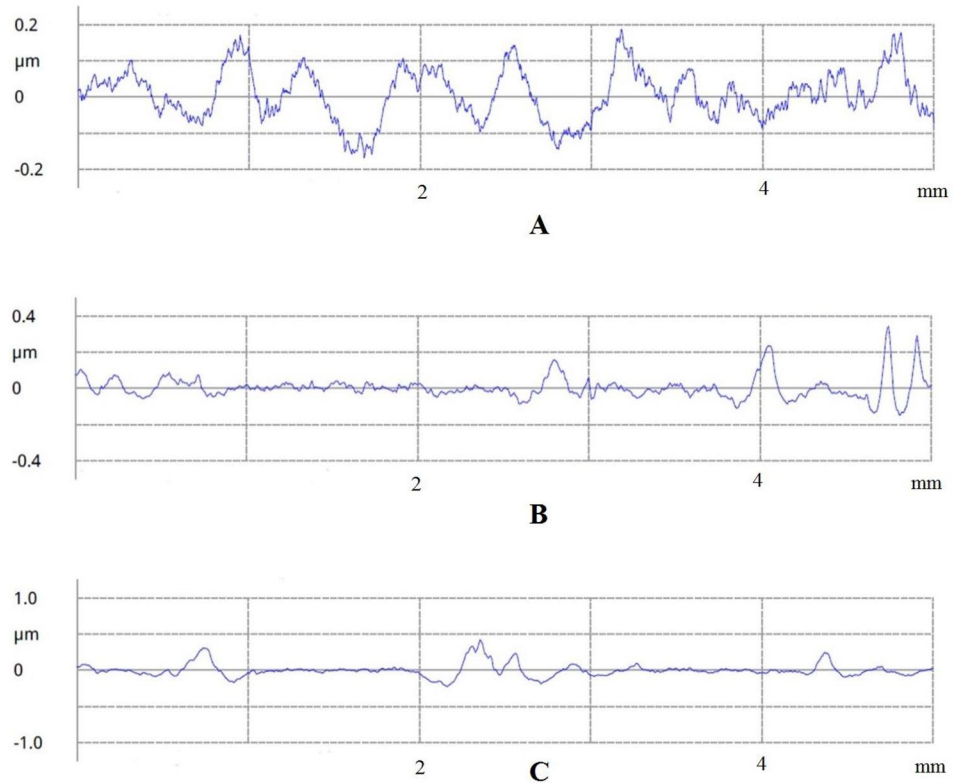


Fig. 20 Surface roughness profile of channels created in conditions of $V=0.6$ mm/min - $U=38$ V, rotational speed of zero and **a** NaOH-20%, **b** NaOH-25% and **c** NaOH-30%

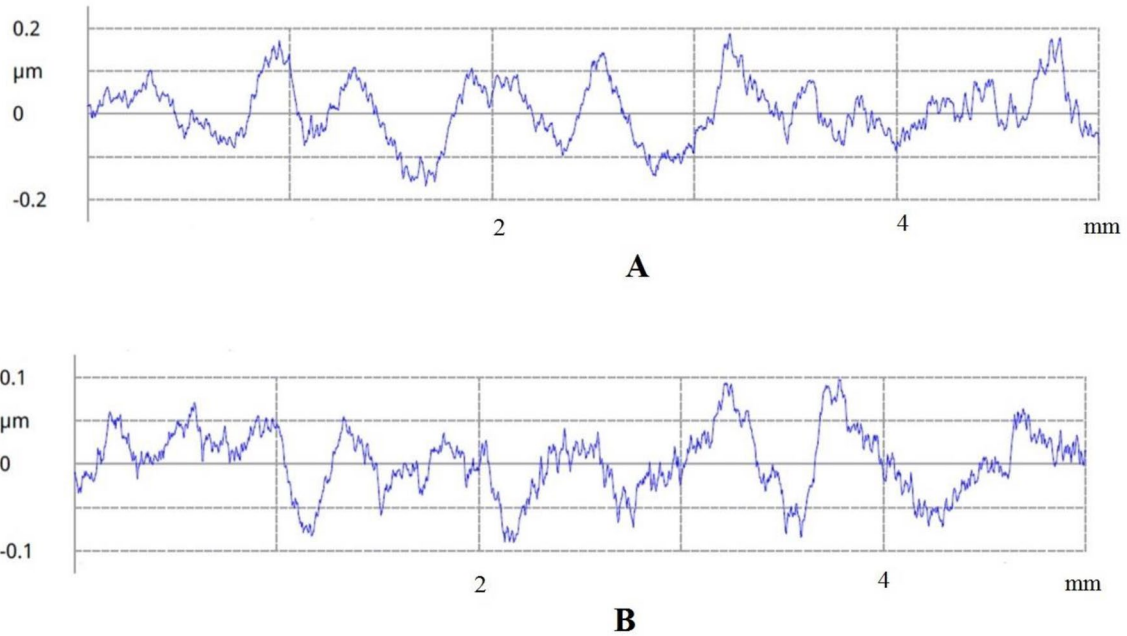
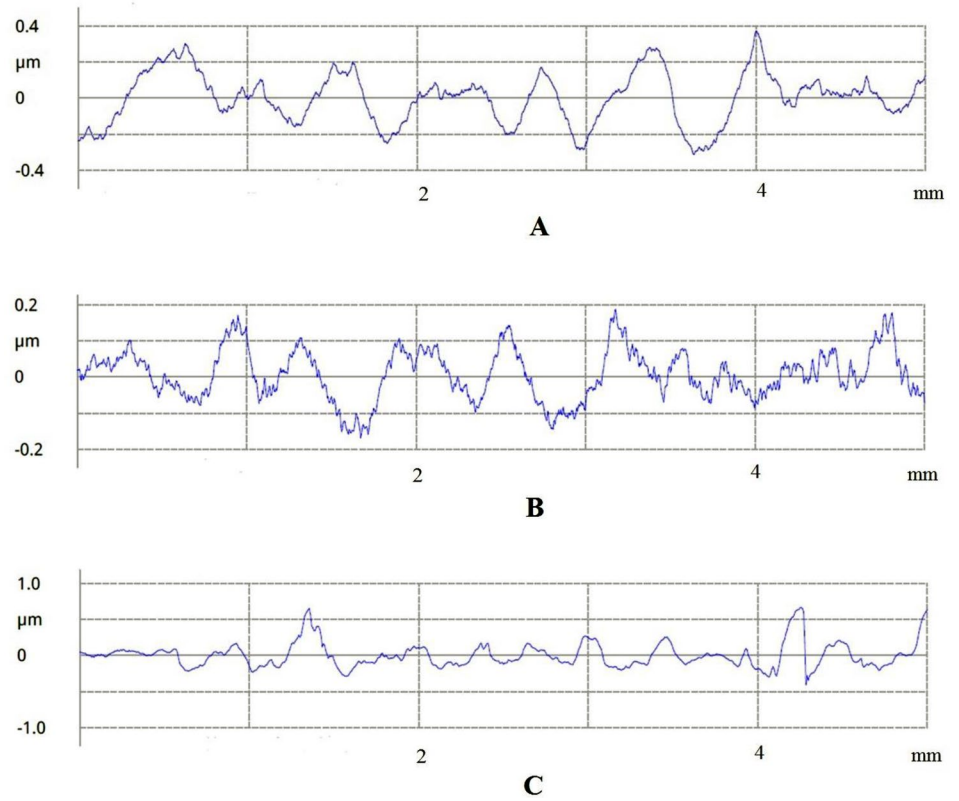


Fig. 21 Surface roughness profile of channels created in conditions of $U=38$ V, NaOH-25%, zero rotational speed and feed rates of **a** $V=0.6$ mm/min and **b** $V=1.2$ mm/min

References

1. Wang J et al (2018) Surface integrity of alumina machined by electrochemical discharge assisted diamond wire sawing. *J Manuf Process* 31:96–102
2. Reichenbach IG et al (2018) Micromachining of PMMA—manufacturing of burr-free structures with single-edge ultra-small micro end mills. *Int J Adv Manuf Technol* 96(9–12):3665–3677
3. Haashir A, Debnath T, Patowari PK (2020) A comparative assessment of micro drilling in boron carbide using ultrasonic machining. *Mater Manuf Process* 35(1):86–94
4. Aaraj Khodaii SJ et al (2018) Optimization of grinding partially stabilized zirconia (PSZ) for dental Implant application. *Modares Mech Eng* 18(7):187–194
5. Khodaii J et al (2019) Surface integrity and flexural strength improvement in grinding partially stabilized zirconia. *J Central South Univ* 26(12):3261–3278
6. Khodaii J et al (2020) Improvement of surface integrity in the grinding of bioceramic partially stabilized zirconia using analytical, numerical, and experimental methods. *Ceram Int*. <https://doi.org/10.1016/j.ceramint.2020.02.168>
7. Whitesides GM (2006) The origins and the future of microfluidics. *Nature* 442(7101):368–373
8. Yi M et al (2018) Fabricating method of SU-8 photoresist conical nozzle for inkjet printhead. *Mater Manuf Process* 33(8):898–904
9. Zainal Abidin NW, Ab Rashid MFF, Nik Mohamed NMZ (2019) A Review of Multi-holes Drilling Path Optimization Using Soft Computing Approaches. *Arch Comput Methods Eng* 26:107–118. <https://doi.org/10.1007/s11831-017-9228-1>
10. Gang MG et al (2019) Wettability modification of cyclic olefin copolymer surface and microchannel using micromilling process. *J Manuf Process* 37:168–176
11. Essa K et al (2017) Manufacturing of metallic micro-components using hybrid soft lithography and micro-electrical discharge machining. *Int J Adv Manuf Technol* 91(1–4):445–452
12. Kam DH, Kim J, Mazumder J (2018) Near-IR nanosecond laser direct writing of multi-depth microchannel branching networks on silicon. *J Manuf Process* 35:99–106
13. Saeidpourazar R et al (2012) A prototype printer for laser driven micro-transfer printing. *J Manuf Process* 14(4):416–424
14. Kandlikar S et al (2005) Heat transfer and fluid flow in minichannels and microchannels. Elsevier, Amsterdam
15. Rattan N, Mulik RS (2017) Improvement in material removal rate (MRR) using magnetic field in TW-ECSM process. *Mater Manuf Process* 32(1):101–107
16. Kumar N, Mandal N, Das A (2020) Micro-machining through electrochemical discharge processes: a review. *Mater Manuf Process* 35(4):363–404
17. Elhami S, Razfar M (2017) Study of the current signal and material removal during ultrasonic-assisted electrochemical discharge machining. *Int J Adv Manuf Technol* 92(5–8):1591–1599
18. Rathore RS, Dvivedi A (2020) Sonication of tool electrode for utilizing high discharge energy during ECDM. *Mater Manuf Process* 35(4):415–429
19. Shamim FA, Dvivedi A, Kumar P (2020) On near-dry wire ECDM of Al6063/SiC/10p MMC. *Mater Manuf Process*. <https://doi.org/10.1080/10426914.2020.1802044>
20. Gupta PK, Dvivedi A, Kumar P (2016) Effect of pulse duration on quality characteristics of blind hole drilled in glass by ECDM. *Mater Manuf Process* 31(13):1740–1748
21. Singh T, Dvivedi A (2020) On prolongation of discharge regime during ECDM by titrated flow of electrolyte. *Int J Adv Manuf Technol* 107(3):1819–1834
22. Zhang C et al (2019) Effect of solution conductivity on tool electrode wear in electrochemical discharge drilling of nickel-based alloy. *Int J Adv Manuf Technol* 103(1–4):743–756
23. Wüthrich R et al (1999) In situ measurement and micromachining of glass. In: MHS'99. Proceedings of 1999 international symposium on micromechatronics and human science (Cat. No. 99TH8478). IEEE
24. Furutani K, Maeda H (2008) Machining a glass rod with a lathe-type electro-chemical discharge machine. *J Micromech Microeng* 18(6):065006
25. Fascio V et al (1999) 3D microstructuring of glass using electrochemical discharge machining (ECDM). In: MHS'99. Proceedings of 1999 international symposium on micromechatronics and human science (Cat. No. 99TH8478). IEEE
26. Yang C et al (2006) Improving machining performance of wire electrochemical discharge machining by adding SiC abrasive to electrolyte. *Int J Mach Tools Manuf* 46(15):2044–2050
27. Mehrabi F et al (2018) Application of electrolyte injection to the electro-chemical discharge machining (ECDM) on the optical glass. *J Mater Process Technol* 255:665–672
28. Sabahi N, Razfar MR (2018) Investigating the effect of mixed alkaline electrolyte (NaOH+ KOH) on the improvement of machining efficiency in 2D electrochemical discharge machining (ECDM). *Int J Adv Manuf Technol* 95(1–4):643–657
29. AarajKhodaii SJ, Rahimi A (2015) Optimization of surface roughness in stereolithography. *Modares Mech Eng* 15(1):245–256
30. Whitehouse DJ (2010) Handbook of surface and nanometrology. CRC Press, Boca Raton
31. Ziki JDA, Didar TF, Wüthrich R (2012) Micro-texturing channel surfaces on glass with spark assisted chemical engraving. *Int J Mach Tools Manuf* 57:66–72
32. Wüthrich R, Ziki JA (2009) Micromachining using electrochemical discharge phenomenon. William Andrew, Oxford
33. Wüthrich R, Hof L (2006) The gas film in spark assisted chemical engraving (SACE)—a key element for micro-machining applications. *Int J Mach Tools Manuf* 46(7–8):828–835
34. Didar TF, Dolatabadi A, Wüthrich R (2008) Characterization and modeling of 2D-glass micro-machining by spark-assisted chemical engraving (SACE) with constant velocity. *J Micromech Microeng* 18(6):065016

Publisher's Note Springer Nature remains neutral with regard to jurisdictional claims in published maps and institutional affiliations.